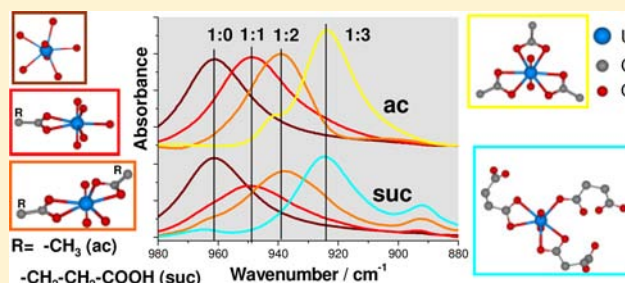


Aqueous Uranium(VI) Complexes with Acetic and Succinic Acid: Speciation and Structure Revisited

Christian Lucks,^{*,†,‡} André Rossberg,^{*,†,‡} Satoru Tsushima,[†] Harald Foerstendorf,[†] Andreas C. Scheinost,^{†,‡} and Gert Bernhard[†][†]Institute of Resource Ecology, Helmholtz-Zentrum Dresden-Rossendorf (HZDR), P.O. Box 510119, 01314 Dresden, Germany[‡]The Rossendorf Beamline at the European Synchrotron Radiation Facility, BP 220, 38043 Grenoble Cedex, France

Supporting Information

ABSTRACT: We employed density functional theory (DFT) calculations, and ultraviolet–visible (UV–vis), extended X-ray absorption fine-structure (EXAFS), and attenuated total reflection Fourier-transform infrared (IR) spectroscopy analyzed with iterative transformation factor analysis (ITFA) to determine the structures and the pH-speciation of aqueous acetate (ac) and succinate (suc) U(VI) complexes. In the acetate system, all spectroscopies confirm the thermodynamically predicted pH-speciation by Ahrlund (1951), with the hydrated uranyl ion and a 1:1, a 1:2 and a 1:3 U(VI)-ac complex. In the succinate system, we identified a new 1:3 U(VI)-suc complex, in addition to the previously known 1:1 and 1:2 U(VI)-suc complexes, and determined the pH-speciation for all complexes. The IR spectra show absorption bands of the antisymmetric stretching mode of the uranyl moiety ($\nu_3(\text{UO}_2)$) at 949, 939, 924 cm^{-1} and at 950, 938, 925 cm^{-1} for the 1:1, 1:2 and 1:3 U(VI)-ac and U(VI)-suc complexes, respectively. IR absorption bands at 1535 and 1534 cm^{-1} and at 1465 and 1462 cm^{-1} are assigned to the antisymmetric $\nu_{3,as}(\text{COO})$ and symmetric $\nu_{3,s}(\text{COO})$ stretching mode of bidentately coordinated carboxylic groups in the U(VI)-ac and U(VI)-suc complexes. The assignment of the three IR bands ($\nu_3(\text{UO}_2)$, $\nu_{3,as}(\text{COO})$, $\nu_{3,s}(\text{COO})$) and the stoichiometry of the complexes is supported by DFT calculations. The UV–vis spectra of the equivalent U(VI)-ac and U(VI)-suc complexes are similar suggesting common structural features. Consistent with IR spectroscopy and DFT calculations, EXAFS showed a bidentate coordination of the carboxylic groups to the equatorial plane of the uranyl moiety for all uranyl ligand complexes except for the newly detected 1:3 U(VI)-suc complex, where two carboxylic groups coordinate bidentately and one carboxylic group coordinates monodentately. All 1:1 and 1:2 complexes have a $\text{U}-\text{O}_{\text{water}}$ distance of ~ 2.36 Å, which is shorter than the $\text{U}-\text{O}_{\text{water}}$ distance of ~ 2.40 Å of the hydrated uranyl ion. For all complexes the $\text{U}-\text{O}_{\text{carboxyl}}$ distance of the bidentately coordinated carboxylic group is ~ 2.47 Å, while the monodentately coordinated carboxylic group of the 1:3 U(VI)-suc complex has a $\text{U}-\text{O}_{\text{carboxyl}}$ distance of ~ 2.36 Å, that is, similar to the short $\text{U}-\text{O}_{\text{water}}$ distance in the 1:1 and 1:2 complexes.



INTRODUCTION

The interaction of uranium(VI) with natural organic matter (NOM) is one of the key parameters determining the fate of uranium in the environment. Knowledge of their aqueous speciation and chemical interactions is hence the basis to model the sorption and transport behavior of uranium(VI). Simple organic acids can serve as model compounds for the carboxylic functionalities of the structurally more complicated NOM. Acetic acid was chosen as model substance because it is the smallest organic acid with a carbon chain and shows for this reason in some aspects similar behavior like all the larger carboxylic acids. Succinic acid was chosen because it has two carboxylic groups that are not so close to each other that larger rings need to be formed for complexation with one metal atom, thereby simulating the assembly of carboxyl groups at the surface of NOM macromolecules.

According to thermodynamic speciation calculations,^{1–5} four U(VI) complexes are expected in U(VI)-acetate system: the

uranyl aquo complex $\text{UO}_2(\text{H}_2\text{O})_5^{2+}$, and the 1:1, 1:2, and 1:3 complexes UO_2ac^+ , UO_2ac_2^0 , and UO_2ac_3^- . Only the first and the last, $\text{UO}_2(\text{H}_2\text{O})_5^{2+}$ and UO_2ac_3^- , are chemically accessible in pure form at very low (pH 0) and slightly acidic (pH 4) pH values, respectively, while the remaining complexes coexist in the intermediate pH range. Thus, the majority of the spectroscopic signals obtained represent a spectral mixture of the signals of the coexisting complexes and only average information can be gained, particularly if the spectral resolution is limited because of method inherent reasons.

Aqueous systems like U-ac have been investigated in the past by Extended X-ray Absorption Fine Structure (EXAFS),^{5,6} Infrared absorption (IR),^{7–9} Raman scattering,^{8,10} and Ultraviolet–visible absorption (UV–vis) spectroscopies. However, these studies show significant disagreement with respect to

Received: July 18, 2012

Published: October 30, 2012

stoichiometry, structure, and speciation. One reason for this might be that the spectral mixtures were not consistently treated with multivariate statistical methods to isolate the pure species. With the aid of factor analysis, the number of acting complexes can be estimated and the spectral mixtures can be decomposed into the spectra of the acting complexes and their pH speciation.¹¹ A typical example is EXAFS spectroscopy, which is a major tool for molecular structural investigations in aqueous solutions. Because of the limited spatial resolution (≥ 0.1 Å), however, structural parameters determined by shell fitting, such as the coordination number (CN), the radial distance (R), and the Debye–Waller factor (DW) as a measure of the thermal and structural disorder, will reflect the weighted average values of all species being present in a sample. If single species cannot be prepared chemically, then iterative transformation factor analysis (ITFA)¹² is a useful tool to decompose the spectra of species mixtures into the spectra of the most prevalent species and their fraction for each spectral mixture. These isolated spectra can then be shell-fitted like experimental spectra to derive the structural parameter of each complex. Conceptually, the ITFA involves three steps. In the first step principal component analysis¹¹ is performed to determine the number of acting metal complexes in the spectral mixtures and to decompose the spectral mixtures into a set of eigenvectors. In the second step the eigenvectors are mathematically transformed by the VARIMAX rotation¹³ into the so-called factor loadings that correlate at most with the unknown relative concentrations of the metal complexes in the spectral mixtures. As a model independent method the VARIMAX rotation uses only the result of the principal component analysis; hence, no further chemical information is needed. In the third step the eigenvectors are transformed into the spectra and the relative concentrations of the complexes by using the iterative target test (ITT).¹⁴ For the ITT some relative concentrations or at least their minima and maxima in the spectral mixtures must be known and used as constraints. The minima and maxima of the relative concentrations are supplied by the VARIMAX rotation.

For EXAFS spectroscopy of uranyl complexes the radial distance between U and the surrounding equatorial oxygens (O_{eq}) is a sensitive parameter to elucidate the coordination of uranium(VI) complexed by carboxylic acids.¹⁵ The coordinating water oxygen can be found at a U– O_{eq} distance of ~ 2.41 Å in the aquo complex.^{16,17} A bidentate coordination of carboxyl groups results in significantly longer U– O_{eq} distances of ~ 2.47 Å (EXAFS;^{5,15} XRD¹⁸). The formation of 5- or 6-membered ring chelates, like with oxalate¹⁹ and malonate,²⁰ reduces the average U– O_{eq} distances to 2.38 Å ($\text{UO}_2\text{ox}_2^{2-}$) and 2.37 Å ($\text{UO}_2\text{mal}_2^{2-}$). Monodentate coordination of carboxylic groups results in U– O_{eq} distances of around 2.28 Å (solid sample¹⁵) or 2.35 Å (aqueous solution⁵). For coordinating carboxylic acids some U–C distances are characteristic for a specific coordination environment. In the case of bidentate coordination of the carboxylic group, the U–C distance at 2.8 Å to 2.9 Å is sometimes detected (EXAFS;^{6,15} XRD¹⁸). Even more pronounced and therefore easier to detect is a multiple scattering path (MS) of the distal carbon (C_{dis}), which generates a strong signal at a distance of around ~ 4.3 Å because of the so-called focusing effect arising from the collinear arrangement of uranium, the carboxylic carbon and the distal carbon atom.¹⁵ In contrast, the absence of any carbon feature around these distances suggests a different mode of coordination like monodentate coordination or ring chelate

formation, where the carbon is located at a distance of about 3.2 Å.^{5,19}

Solid uranyl complexes with carboxylic ligands might be a way to avoid the problem of their aqueous analogues, which often occur only as mixtures. However, the structure of the solid and aqueous analogues are not necessarily the same: While Denecke et al.¹⁵ identified only bidentate carboxylate coordination for the solid trisacetato complex, Jiang et al.⁵ identified two bidentately and one monodentately coordinated carboxyl groups for the aqueous trisacetato complex. Additionally, a ternary hydroxo complex $[\text{UO}_2\text{ac}_3\text{OH}]^{2-}$ was suggested to be formed at $\text{pH} > 4$. This complex was postulated to have one bidentately and two monodentately coordinated acetate groups. The 1:1 and 1:2 U-ac complexes were proposed to have exclusively bidentate coordinated carboxyl groups although the authors admitted in the case of the 1:2 complexes that the results were not unambiguous because the complexes were mixed together in the investigated solutions.

Bailey et al. found an increase in the radial U– O_{eq} distance from 2.42 Å to 2.44 Å in the pH range of $\text{pH} 1.8$ to $\text{pH} 3.2$ and a decrease from $\text{CN} = 4.6$ to $\text{CN} = 3.8$.⁶ They interpreted this data as an evidence for UO_2ac_2^0 having two bidentately coordinated acetate ligands and no coordinated water molecules. Although the used uranium concentrations were between 50 mM and 100 mM, the data was of low quality, and the interpretations are doubtful because a 4-fold coordination of uranium(VI) would result in much lower U– O_{eq} distances²¹ than observed.

Infrared absorption spectroscopy is another powerful tool for the discrimination of monodentate and bidentate coordination of carboxyl groups. The mode of coordination has a significant impact on the doubly degenerated stretching vibration mode of this functional group, that is, $\nu_3(\text{COO})$. In the spectrum of the free ligand this mode is split into an antisymmetric ($\nu_{3,\text{as}}(\text{COO})$) and a symmetric ($\nu_{3,\text{s}}(\text{COO})$) stretching mode. In the case of monodentate coordination, the splitting ($\Delta\nu$) increases compared to the free ligand, whereas it decreases for bidentate coordination.^{7,8,22} Kakahana et al.⁷ identified for a large number of U(VI) complexes with different carboxylic acid $\Delta\nu$ values of ~ 202 – 226 cm^{-1} for monodentate coordination, $\Delta\nu \sim 172$ – 204 cm^{-1} for the free ligand and $\Delta\nu \sim 58$ – 80 cm^{-1} for bidentate coordination.⁷ For bidentate U-ac complexes the following band positions were given: $\nu_{3,\text{as}}(\text{COO})$: 1527,⁸ 1537,⁹ and 1538 cm^{-1} ; $\nu_{3,\text{s}}(\text{COO})$: 1466,⁸ 1472,⁹ and 1467 cm^{-1} .⁷ In the case of monodentate coordination, the following band positions were identified: $\nu_{3,\text{as}}(\text{COO})$: 1603⁹ and 1595 cm^{-1} ;⁸ $\nu_{3,\text{s}}(\text{COO})$: 1390⁹ and 1389 cm^{-1} .⁸ However, these assignments for monodentate coordination were not confirmed by other spectroscopic techniques.

An increasing number of ligand molecules coordinated in the equatorial shell of the uranyl moiety lowers the frequency of the antisymmetric stretching vibration. Consequently, for the aqueous uranyl ion $[\text{UO}_2(\text{H}_2\text{O})_5]^{2+}$, later on referred to as uranyl hydrate, the absorption band is observed at 962 cm^{-1} , whereas it is observed at 954 and 928 cm^{-1} for the 1:1 and 1:2 complex, respectively. For the 1:3 complex no assignment was possible.⁸ However, the frequency of the $\nu_3(\text{UO}_2)$ mode gives no direct link to the mode of coordination.

Furthermore, the results of different IR investigations show inconsistencies. Whereas Kakahana et al.⁷ found no evidence of monodentate coordination, Quiles et al.⁸ identified it for UO_2ac^+ and UO_2ac_2^0 . No conclusion could be drawn on the 1:3 complex by the latter authors, since they did not use acetate

in excess, and the 1:3 complex was formed to a minor extent only.

A different way to analyze the 1:3 complex was provided by Groenewold.²³ The trisacetato complex was generated and isolated using different kinds of mass spectrometry, and then analyzed using the infrared multiphoton dissociation (IRMPD) technique. The spectra recorded were interpreted with the aid of DFT calculations. It was concluded that one monodentately and two bidentately coordinated acetates form the trisacetato complex. Note, however, that by applying this technique the 1:3 complex is transferred into the gas phase; hence, there remains some ambiguity whether this structure is truly representative of that in solution.

Only a small number of works are dedicated to the structural study of the interaction of uranium(VI) with succinic acid in aqueous solution. Especially EXAFS spectroscopy has not been applied to this system until now.

Bismondo et al.²⁴ performed calorimetric and potentiometric measurements to obtain complex stability constants, enthalpies and entropies of reaction. The following complexes were identified: UO_2Hsuc^+ , UO_2suc^0 , $\text{UO}_2\text{Hsuc}_2^-$ (suc is a common acronym for the doubly deprotonated succinic acid). Bismondo et al. stressed the possibility that succinic acid may form a seven membered ring with U(VI). Such a chelate structure was proposed for UO_2suc^0 and $\text{UO}_2\text{Hsuc}_2^-$ according to the free energy, enthalpy and entropy changes. As in the case of the U-ac system the 1:1 complex can not be prepared as predominant species assuming uranium concentrations accessible with EXAFS. In contrast, the 1:2 U-suc complex can have a fraction of up to 95% in solution.²⁴ A very recent paper by Rawat et al.²⁵ applied on the U-suc system came to the conclusion that over the pH range of 1.5 to 4.5 only the 1:1 complex is formed based on potentiometry and isothermal titration calorimetry. The differences between both works are mainly due to the lower concentration of succinate used by Rawat et al.²⁵ (up to 83 mM at $[\text{U}] = 5 \text{ mM}$) compared to Bismondo et al.²⁴ (up to 350 mM at $[\text{U}] = 10 \text{ mM}$). The applied uranium(VI) concentrations are comparable with the concentrations used in the present investigation.

In this study, pH series of uranium(VI) in the presence of a large excess of acetic and succinic acid were systematically investigated using UV-vis, EXAFS and IR spectroscopy coupled with ITFA and DFT calculations. A large excess of organic ligand was necessary to avoid the formation of hydroxo complexes of the uranyl ion and also the ternary uranyl-carboxylate-hydroxo complexes. Moreover, the utilization of this multitude of techniques and especially a consequent implementation of ITFA (see Supporting Information) enables structural analysis even in multicomponent systems. The results of this study may help to understand these systems in more detail regarding the difficulties in analyzing spectra of mixed complexes.

■ EXPERIMENTAL SECTION

Sample Preparation. All reagents used were of analytical grade. $\text{UO}_3 \cdot x\text{H}_2\text{O}$ (synthesized by thermal decomposition of $\text{UO}_2(\text{NO}_3)_2 \cdot 6\text{H}_2\text{O}$) was first dissolved in 0.5 M perchloric acid (HClO_4) to yield a 0.1 M uranium stock solution (concentration controlled by ICP-MS). Both acetic and succinic acid were added as water free compounds. The pH was adjusted using NaOH and HClO_4 or HCl in the case of IR measurements. A SenTix Mic electrode was used to measure pH with a precision of ± 0.05 pH units.

EXAFS Spectroscopy. For the aqueous samples of the U-ac system and the U-suc system, the concentrations were $[\text{U}] = 0.05 \text{ M}$

and $[\text{ac}] = 1 \text{ M}$ and $[\text{U}] = 0.02 \text{ M}$ and $[\text{suc}] = 0.25 \text{ M}$, respectively. In the case of the U-ac system, precipitations were observed at the two highest pH values which were allowed to settle down before the measurements. For these two solutions a final concentration of $[\text{U}] = 0.036 \text{ M}$ at pH 3.62 and $[\text{U}] = 0.028 \text{ M}$ at pH 3.86 was measured. Each solution was filled in polyethylene cuvettes and was heat sealed. Uranium L_{III} -edge measurements of the samples were done in transmission (U-ac) or fluorescence (U-suc) mode using ion chambers or a 13-element Ge detector, respectively, at the Rossendorf Beamline BM20²⁶ (ROBL), ESRF, France. For energy calibration, an yttrium foil was measured simultaneously in transmission mode. The program suite EXAFSPAK²⁷ was used for averaging, deadtime correction, energy calibration, isolation of the EXAFS signal, and data fitting. The ionization energy (E_0) was set to $E_0 = 17185 \text{ eV}$ for all spectra. For data fitting, theoretical phase and amplitude functions were calculated based on EXAFS data of $\text{Na}[\text{UO}_2\text{ac}_3]_{(s)}$ ¹⁵ and aqueous U(VI) acetate solutions⁵ using FEFF 8.20.²⁸ The model is shown on Supporting Information, Figure S12.

UV-vis Spectroscopy. The same aqueous U-ac solutions as prepared for the EXAFS measurements were used for UV-vis measurements. The absorption of the spectra of the last two samples with the highest pH values were corrected according to the decreased uranium concentration due to precipitation. In the case of the U-suc system a UV-vis pH titration experiment from the near neutral to the acidic pH range was performed by adding stepwise concentrated HClO_4 to a solution of 10 mM U(VI) with 0.25 M suc, while the volume increase (smaller than 5%) was considered as a change in concentration. The UV-vis spectra were measured using a Varian Cary 5g spectrophotometer in the spectral range from 700 to 350 nm. The absorbance data was recorded in a 10 mm quartz cuvette against Milli-Q water in double beam mode. An averaging time of 0.1 s and an interval of 0.2 nm were applied. All spectra were corrected to zero at 700 nm.

IR Spectroscopy. Infrared absorption spectroscopy was applied on both systems using the molar concentrations as used for the UV-vis measurements. For pH adjustment, concentrated HCl and NaOH was used. The spectra were recorded on a Bruker Vertex 80/v instrument. The background correction was done by subtraction of the spectrum of an acetate or a succinate solution with the corresponding pH and acid concentration. The spectra were averaged and subtracted using the OPUS software package (Bruker, Ettlingen, Germany). Finally, the spectra were corrected to zero by subtraction of the offset at 1100 cm^{-1} where no absorption occurs in all spectra recorded. For the application of ITFA in the range of the $\nu_3(\text{UO}_2)$ band a second baseline correction was done between 700 and 1100 cm^{-1} . For this correction, a spline function was used consisting of three consecutive functions: a third order polynomial for the pre peak area, a linear function for the peak and another third order polynomial for the post peak area.

DFT Calculations. All the calculations were performed using Gaussian 03.²⁹ Structures were optimized in aqueous phase at the B3LYP level by using the CPCM solvation model³⁰ with UAHF³¹ radii. The energy-consistent small-core effective core potential (ECP) and the corresponding basis set suggested by Dolg et al. were used for uranium,³² carbon,³³ and oxygen.³⁵ The d-function on oxygen and the g-function on uranium were included. Moreover, the most diffuse basis functions on uranium with the exponent 0.005 (all s, p, d, and f type functions) were omitted during the geometry optimization, which made the convergence of the electronic wave function much faster, and had only little effect (less than 1 kJ/mol) on the total energy.³⁴ For hydrogen we used the 5s functions contracted to 3s.³⁵ The Gibbs energy correction to the electronic energy was calculated at the B3LYP level from the vibrational energy levels in aqueous phase and the molecular partition functions. The structures were confirmed to be energy minima through vibrational frequency analysis where no imaginary frequency was found to be present.

RESULTS AND DISCUSSION

IR Spectroscopy. Figure 1 shows the IR spectra of the aqueous U-ac solutions recorded at pH values ranging from pH 0.86 to pH 3.77 in the spectral range of the $\nu_3(\text{UO}_2)$ mode.

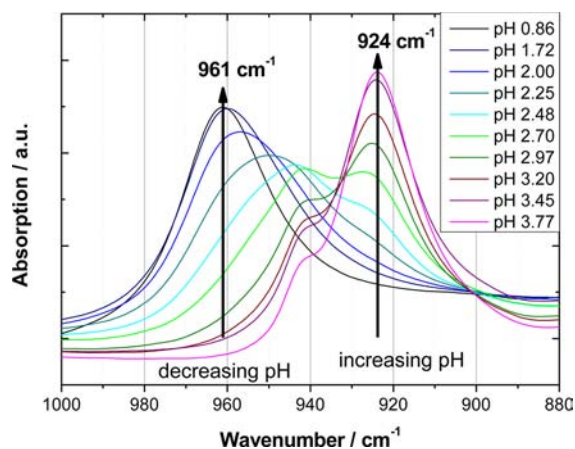


Figure 1. IR spectra of the uranyl region ($\nu_3(\text{UO}_2)$) of the U-ac system, arrows indicating the direction of pH changes and the final band position.

A large frequency shift of the $\nu_3(\text{UO}_2)$ mode from 961 to 924 cm^{-1} is observed with increasing pH. A similar shift of the $\nu_3(\text{UO}_2)$ mode from 961 to 925 cm^{-1} is observed for the U-suc system (Figure 3). This red shift can be explained by an increased fraction of uranyl ions complexed by acetate or succinate ligands at higher pH values, compared to the free aquo complex at lower pH values. Contributions from hydroxo complexes to the spectra, which are expected to show similar shifts of the $\nu_3(\text{UO}_2)$ mode in the same frequency range,³⁶ can be neglected because of large excess of the organic ligands.

At the lowest pH, uranyl hydrate is the dominant species in solutions of both systems showing an absorption band at 961 cm^{-1} . At the highest pH, the 1:3 U-ac and the 1:2 succinate complexes are predicted to become predominant according to the speciation calculations.^{1,24} Interestingly, these complexes that might have different stoichiometries according to the literature cited above show the same spectral positions of the $\nu_3(\text{UO}_2)$ mode. For a comprehensive evaluation of the spectral data set recorded throughout the whole pH range, ITFA was applied to study the correlations between the observed frequencies of the $\nu_3(\text{UO}_2)$ modes and the prevailing pH for both U-ac and U-suc systems.

As a first step, the principal component analysis of the IR spectra was performed in the spectral range of $\nu_3(\text{UO}_2)$ peak, which suggested the presence of four distinct components in both the U-ac and the U-suc systems. As a second step, the VARIMAX rotation¹³ provided model-independent factor loadings (Figure 2-A and Figure 2-B) which correlate at most with the unknown relative concentrations of the present U(VI) complexes (see Supporting Information). In the case of the U-ac system, the factor loadings, as a qualitative measure of the relative concentrations, are in good agreement with the speciation calculation using the complex stability constants published by Ahrlund¹ (Figure 2-A,C). In particular, the maxima of the factor loadings were in good agreement with those of the relative concentrations of the components derived by the thermodynamic speciation calculation, suggesting that the determined components correspond to the proposed

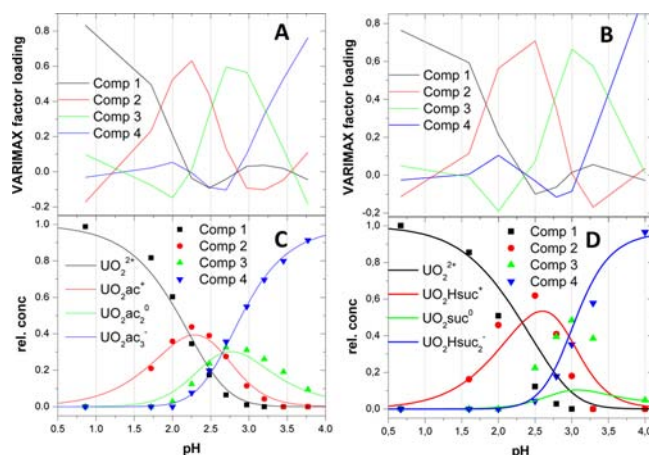


Figure 2. ITFA results gained from the IR spectra of the U-ac (left panel) and U-suc system (right panel). VARIMAX factor loadings of the components (top), ITT calculated species distribution of the components (bottom, dots) and thermodynamic speciation calculation^{1,24} (bottom, solid lines).

complexes.¹ As a third step, the relative concentrations of the components were calculated with ITT (Figure 2-C). Again, a good agreement with the results of the thermodynamic speciation calculation is found for the U-ac system, whereas for the U-suc system strong deviations between the calculated speciation based on literature data²⁴ and the results derived from ITFA were observed (Figure 2-D), especially regarding the third occurring species with increasing pH, UO_2suc^0 .

The IR spectra of the single components derived from ITFA (Figure 3) reproduce the observed frequency shift of the $\nu_3(\text{UO}_2)$ mode with rising pH (Figure 1). For both systems

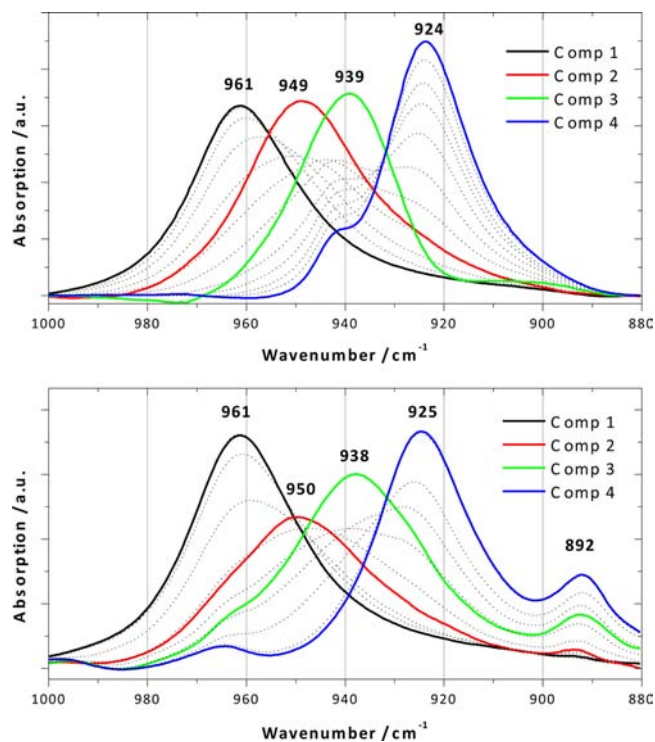


Figure 3. ITFA extracted IR component spectra (solid lines) and experimental data (dotted lines) of the U-ac (top) and U-suc system (bottom).

Table 1. DFT Calculated Major Interatomic Distances (in Å) and Vibrational Frequencies of the $\nu_3(\text{UO}_2)$ Mode (in cm^{-1}) for UO_2^{2+} , UO_2ac^+ , UO_2ac_2^0 , and UO_2ac_3^- Complexes

	mode	U–O _{ax}	R(U–O _{carboxyl})	R(U–O _{water})	U–C	$\nu_3(\text{UO}_2)$
UO_2^{2+}	CN = 5	1.754 × 2		2.412, 2.487, 2.420, 2.417, 2.486		975.8
UO_2ac^+	Bi, CN = 5	1.763, 1.764	2.427, 2.421	2.434, 2.456, 2.437	2.832	956.2
	Bi, CN = 6	1.763, 1.764	2.473, 2.474	2.544, 2.553, 2.555, 2.525	2.893	954.7
	Mono, CN = 5	1.766, 1.766	2.253, 3.875	2.473, 2.529, 2.465, 2.461	3.432	948.6
UO_2ac_2^0	Bi, CN = 5	1.770 × 2	2.425, 2.441, 2.439, 2.426	2.439	2.834, 2.835	942.7
	Bi, CN = 6	1.773 × 2	2.477, 2.482, 2.484 × 2	2.515, 2.516	2.891, 2.888	934.7
UO_2ac_3^-	Bi, CN = 6	1.779, 1.781	2.498, 2.494 2.496 × 4		2.901 × 3	921.5

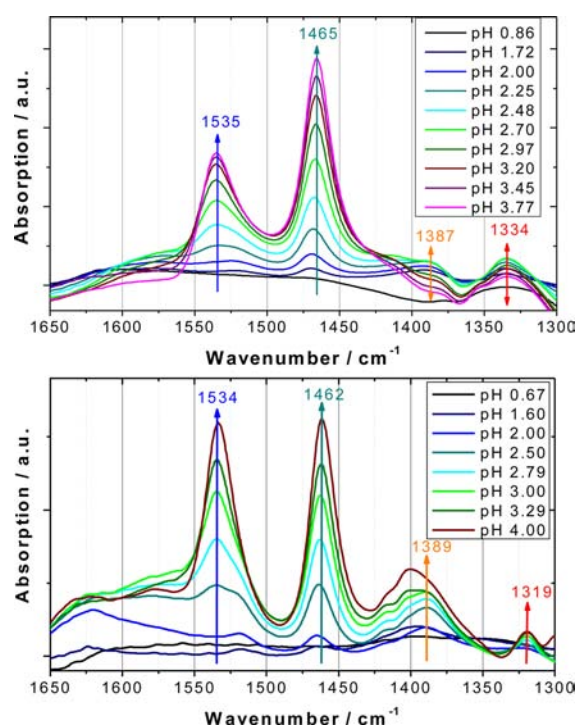
and for the components 1 to 4 a systematic bathochromic shift of the peak maximum is visible representing an increase of the number of coordinated ligand molecules. This observation supports the assignment of the single components 1 to 4 to the corresponding 1:0, 1:1, 1:2 and the 1:3 complexes, respectively. Moreover, all component spectra (Figure 3) show approximately a Gaussian shape so that each single component may represent a distinct complex stoichiometry.

In the U-suc system, the frequencies of the maxima of the single component spectra are nearly identical to those found for the U-ac system (Figure 3, Supporting Information, Table S2), suggesting the presence of complexes with the same stoichiometries as in the U-ac system. This relationship between stoichiometry and the frequency of the $\nu_3(\text{UO}_2)$ mode will later be evidenced by the results of DFT calculations. Consequently, the U-suc complexes found at pH ~ 3 and at the highest pH, referred to as component 3 and component 4, represents most likely 1:2 and 1:3 complexes, respectively. This is opposite to the literature data²⁴ where the competing species were 1:1 and 1:2 complexes.

It has to be noted that the calculated spectra of the 1:3 complexes also show a spectral feature which can not be attributed to the $\nu_3(\text{UO}_2)$ mode. In the U-ac and U-suc systems, shoulders at 942 cm^{-1} and 892 cm^{-1} are observed, respectively. In the case of the U-ac series the spectral feature at 942 cm^{-1} is not apparent in the component spectra of the 1:1 and 1:2 U-ac complexes because of the strongly interfering $\nu_3(\text{UO}_2)$ mode and low intensity. In the respective spectra of the U-suc series, the spectral feature at 892 cm^{-1} shows increasing intensity with increasing number of coordinating ligands. Because of this observed correlation, the assignment to contributions from the succinic ligand (most probably the $\nu(\text{CC})$ mode) has been suggested.³⁷

In general, the red shift of the $\nu_3(\text{UO}_2)$ mode in uranyl complexes is due to the weakening of the axial(ax) U–O_{ax} bond because of the σ and/or π contribution from the ligands, which is in turn usually accompanied by an elongation of the U–O_{ax} bond length.³⁸ Consequently, the coordination of acetate ligands leads to a systematic lengthening of the U–O_{ax} distances and a red shift of the $\nu_3(\text{UO}_2)$ band which is confirmed by EXAFS results (Table 2) and DFT calculations (Table 1).

In addition to the frequency range of the $\nu_3(\text{UO}_2)$ mode, the symmetric and antisymmetric stretching modes of the carboxyl groups, that are $\nu_{3,\text{as}}(\text{COO})$ and $\nu_{3,\text{s}}(\text{COO})$, respectively, provide further information on the coordination mode of the ligand to the uranyl ion. The spectral splitting of these bands ($\Delta\nu$), which can be observed in the spectral region between 1650 and 1300 cm^{-1} (Figure 4), allows a discrimination of bidentate and monodentate coordination.^{7,22} Generally, a bidentate coordination is characterized by a splitting to a

**Figure 4.** IR spectra in the carboxylate region of the U-ac (top) and the U-suc system (bottom), arrows indicate increasing pH.

lower extent ($<100\text{ cm}^{-1}$) whereas a monodentate binding of a carboxyl group to the uranyl ion results in a spectral splitting larger than 150 cm^{-1} .⁷ The vibrational modes of the carboxyl group of the acetate ligand have nearly the same frequency values throughout the whole pH range investigated (Figure 4), that are 1535 cm^{-1} for the $\nu_{3,\text{as}}(\text{COO})$ and 1465 cm^{-1} for the $\nu_{3,\text{s}}(\text{COO})$ mode. Therefore, in the series of the U-ac spectra (Figure 4), the constant value $\Delta\nu$ of $\sim 70\text{ cm}^{-1}$ discounts the monodentate coordination of the carboxyl groups.

The respective spectra of the U-suc complexes show a similar behavior with increasing pH. The frequencies of the carboxylate bands are almost identical to the ones of the U-ac system (Figure 4). The spectral splitting $\Delta\nu \sim 72\text{ cm}^{-1}$ is indicative of bidentate coordination being the dominant mode of coordination. At pH values ≥ 3 , however, the spectra show a slightly increased absorption in the spectral region around 1580 cm^{-1} and particularly at 1400 cm^{-1} . Assuming that these spectral features represent a small fraction of carboxyl groups, a $\Delta\nu$ value of about 180 cm^{-1} can be derived. Such a degree of splitting would indicate contributions from a monodentately coordinated carboxyl group. Note that because of the interferences with strong modes of the water molecules at higher frequencies and of the hydrocarbon backbone below

1420 cm^{-1} , an unequivocal identification of these modes is not possible.

The absorption changes below 1400 cm^{-1} (Figure 4) can be attributed to modes of the methyl and the CH_2 groups of the acetate and succinate ligand, respectively, undergoing structural alterations upon complexation with the uranyl ion.

DFT Calculations. To obtain information about the coordination number and the mode of coordination in the equatorial shell of the uranyl, the DFT-calculated $\nu_3(\text{UO}_2)$ frequency (Table 1) versus the experimentally determined values are given in Figure 5. Note that there is a systematic

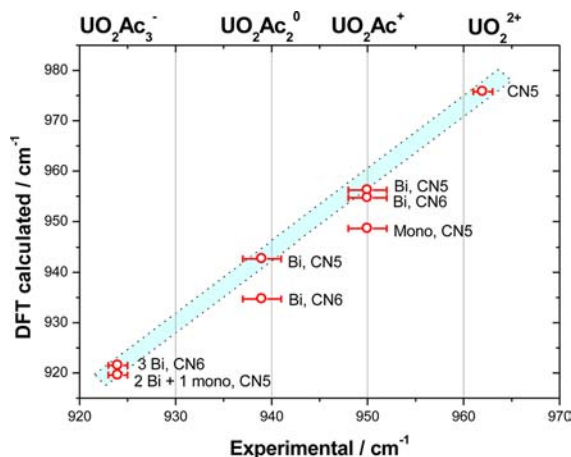


Figure 5. Comparison of DFT calculated band positions of the antisymmetric stretching mode of the uranyl moiety and experimentally observed values in the U-ac system.

discrepancy between theory and experiment because DFT-based vibrational frequency calculations assume harmonic motion of molecular vibration which typically overestimates the frequency values by 5 to 10%. But, their relative difference ($\Delta\nu$) is reasonably assumed to be accurate enough to discriminate bidentate coordination having small band splitting ($\sim 70 \text{ cm}^{-1}$) from monodentate coordination, which has greater band splitting ($\sim 250 \text{ cm}^{-1}$). A linear correlation between theoretical and experimental values for the uranyl symmetric stretching vibrational frequencies has been demonstrated for the various uranyl organic and inorganic complexes in a previous DFT study. Wrong coordination number or wrong mode of coordination can be ruled out when the plot deviates from the linear fitting.³⁸ In the case of the 1:2 U-ac complex the correlation, shown in Figure 5, affirms a coordination number of 5. The coordination number of the 1:1 U-ac complex is 5 as well because CN can only increase with rising number of coordinated acetates (CN = 5 for uranyl hydrate and CN = 6 for 1:3 complex) because for a 6-fold coordination more angular space needs to be provided by the coordination of groups like acetate that have an O–U–O angle smaller than 60° .³⁹ Furthermore, in the 1:1 complex, bidentate coordination is more likely than monodentate coordination (Figure 5). For U-ac and U-suc complexes with the same stoichiometry the DFT calculated $\nu_3(\text{UO}_2)$ frequency is similar (Supporting Information, Table S2).

DFT calculations of the bidentately coordinated complexes show double bands at 1420–1450 cm^{-1} that are assigned to $\nu_{3,s}(\text{COO})$. Furthermore, weaker double bands at 1500–1510 cm^{-1} are assigned to $\nu_{3,as}(\text{COO})$. $\Delta\nu$ ranges from 58 to 72 cm^{-1} which is in excellent agreement with the experimentally

found value of 70 cm^{-1} . For a monodentate 1:1 complex, two strong absorption bands at 1312 and 1562 cm^{-1} are calculated for the $\nu_{3,s}(\text{COO})$ and $\nu_{3,as}(\text{COO})$ mode, respectively; hence, a much larger $\Delta\nu$ value of 250 cm^{-1} is predicted for monodentate coordination. Taking into account that the difference between DFT calculated and measured band position is in the case of monodentate coordination similar ($\sim 25 \text{ cm}^{-1}$) to the difference observed for bidentate coordination, both a band around 1590 cm^{-1} and a band around 1340 cm^{-1} are expected. The first band is not observed, and the absorption band detected at 1334 cm^{-1} (Figure 4), which was previously assigned to the $\delta(\text{CH}_3)$ mode of the methyl group, shows only low intensity and therefore can hardly be attributed to a $\nu_{3,s}(\text{COO})$ mode. Thus, a monodentate coordination contribution to the U-ac complexes can be ruled out.

ITFA of UV–vis Spectra. ITFA was performed on UV–vis spectral series of both U-ac (Supporting Information, Figure S5) and U-suc (Supporting Information, Figure S6) systems to identify the number of spectroscopically distinct complexes, their spectra (Figure 6), and their pH speciation (Supporting

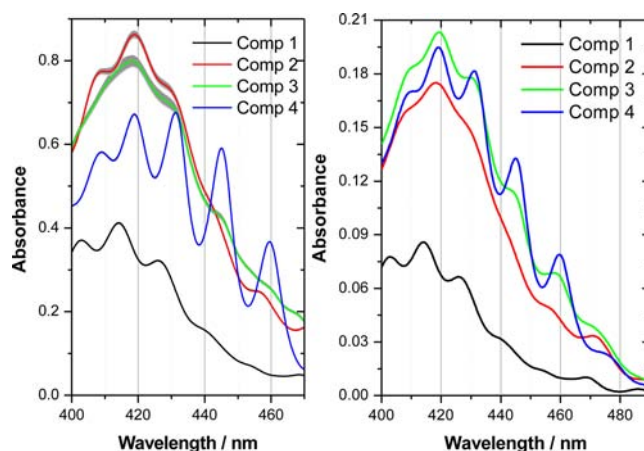


Figure 6. ITFA extracted UV–vis component spectra of the U-ac (left panel) and U-suc system (right panel). Gray regions in the left panel indicate the estimated error by using the method of Roscoe et al.⁴⁰ of the component spectra in the case of the U-ac system.

Information, Figure S7). For both systems, and in line with the results gained by IR, four components were detected. Because of the high data quality of the UV–vis series we expect a low error in determination of the component spectra and the relative concentrations of the components. Therefore, the ITFA results of the UV–vis series can be taken as a proof of the calculated thermodynamical speciations. We estimated the error in determination of the component spectra by using the method of Roscoe et al.⁴⁰ As an example the error in determination of the component spectra is shown in Figure 6 for the U-ac system. It is obvious that the higher the fraction of a component in the pH series, the lower is the error in determination of its spectrum (compare Figure 6 with Supporting Information, Figure S7-C).

The ITT calculated speciation and the speciation based on literature data¹ show a good agreement with an overall standard deviation of 3% (Supporting Information, Figure S7-C) for the U-ac system. Moreover the determined pH speciation is in good agreement with that observed in the IR study (Figure 2-C), hence components 1, 2, 3, and component 4 can be

assigned to the uranyl hydrate, the 1:1, 1:2, and the 1:3 U-ac complexes, respectively.

As in the case of both systems, the spectrum of component 1, exclusively observed in the lower pH range, is identical to the spectrum of an aqueous solution of $\text{UO}_2(\text{ClO}_4)_2$ at low pH; hence, also for the U-suc system component 1 represents uranyl hydrate which is additionally supported by the good agreement of the ITT calculated speciation of component 1 with the speciation gained from the IR measurements (compare Supporting Information, Figure S7-D with Figure 2-D). Also the ITT calculated speciation of the remaining three components match well the speciation determined from the IR spectra for which the components 2, 3, and component 4 were assigned to the 1:1, 1:2, and the 1:3 U-suc complexes. Consequently the ITFA isolated spectra of the components 1, 2, 3, and 4 represents for both systems the spectra of the uranyl hydrate, the 1:1, the 1:2 and the 1:3 complexes, respectively. This assignment can be partially gained by comparing the spectral similarity of the components. For both systems the spectrum of component 1 is nearly identical, the spectrum of component 2 shows a similar UV-vis absorption spectrum (Figure 6) without a maximum neither at 445 nm nor at 460 nm, the spectrum of component 3 and component 4 show maxima at 445 and 460 nm, while the intensities of these characteristic peaks are different for both systems and the spectrum of component 4 shows the strongest variations for both systems. Hence, by taking the assignments of the IR study into account the spectral similarity of the components is higher for U-ac and U-suc complexes with the same stoichiometry.

EXAFS Spectroscopy. At first, shell fitting was performed to all EXAFS spectra of the U-ac (Supporting Information, Figure S9) and the U-suc system (Supporting Information, Figure S10) by introducing only four shells, namely, the O_{ax} , O_{eq} , C single scattering (SS) paths and the 2-legged degenerated 4-legged multiple scattering path ($\text{MS}_{\text{O}_{\text{ax}}}$) along the uranyl chain ($\text{O}_{\text{ax}(1)}\text{-U-O}_{\text{ax}(2)}$). From these shell fits the relative change of the U-O_{eq} and U-C distances can be deduced which allow the estimation of the dominating mode of coordination. In the fitting procedure the CN of $\text{MS}_{\text{O}_{\text{ax}}}$ path was set to the CN of O_{ax} which was kept constant at $\text{CN} = 2$ during the fit, while the DW of the $\text{MS}_{\text{O}_{\text{ax}}}$ path was set to twice the DW of the freely fitted DW of O_{ax} . In the case of the U-ac system, for each spectrum the CNs of O_{eq} and C were calculated by using the thermodynamic speciation calculation¹ and the most probable coordination numbers of the U(VI) complexes deduced from the DFT calculation. These CN were then held constant during the shell fit. We assumed the following distribution of $\text{CN}(\text{O}_{\text{eq}}):\text{CN}(\text{C})$ for the complexes: 5:0 (uranyl hydrate), 5:1 (1:1 U-ac), 5:2 (1:2 U-ac), 6:3 (1:3 U-ac). In the case of U-suc the CN of O_{eq} and C were calculated for each spectrum by using the pH speciation determined by IR spectroscopy and assuming the following $\text{CN}(\text{O}_{\text{eq}}):\text{CN}(\text{C})$ distribution: 5:0 (uranyl hydrate), 5:1 (1:1 U-suc), 5:2 (1:2 U-suc), 5:2 (1:3 U-suc). For both systems, the DW of C was held constant at 0.0042 \AA^2 , the value determined by a shell fit of the ITFA isolated spectrum of the 1:3 U-ac complex (Table 2). For each spectrum the shift in the threshold energy, ΔE_0 , was first allowed to float. With increasing pH the determined ΔE_0 shows a trend to higher values (Supporting Information, Figure S8). Because of the experimental error this trend is not smooth and therefore ΔE_0 was recalculated as a function of the number of coordinated ligands derived from the thermodynamic speciation calculation (for U-ac) or from the

Table 2. Shell Fit Parameters for the Extracted Components in the U-ac System

	atom	CN ^a	R [\AA] ^b	σ^2 [\AA^2] ^c	ΔE_0 [eV] ^d
component 1	O_{ax}	2*	1.764(1)	0.0013(1)	3.9(3)
	O_{eq}	5.1(3)	2.403(3)	0.0067(5)	/3.9
component 2	O_{ax}	2*	1.771(1)	0.0012(1)	4.4(4)
	O_{eq}	5.3(4)	2.411(5)	0.011(1)	/4.4
	C	1.4(3)	2.89(1)	0.0042*	/4.4
component 3	O_{ax}	2*	1.780(1)	0.0014(1)	4.9(3)
	O_{eq}	5.8(3)	2.472(3)	0.0071(5)	/4.9
	C	3.3(3)	2.880(5)	0.0042*	/4.9
	C_{dis}	/3.3	4.362(8)	0.00645*	/4.9

^aCoordination number. ^bInteratomic distance. ^cDebye–Waller factor. ^dThreshold energy, * fixed parameter, parameter linked proportional to the parameter in the row above. $\text{CN} \pm \sim 20\%$, $R \pm \sim 0.02 \text{ \AA}$. The standard deviations of the variable parameters as estimated by EXAFSPAK are given in parentheses. $\text{MS}_{\text{O}_{\text{ax}}}$ and both $\text{MS}_{\text{O}_{\text{ax}}}$ paths of C_{dis} were linked to the structural parameters of O_{ax} and $\text{SS}_{\text{C}_{\text{dis}}}$ accordingly.

ITT calculated speciation by using the IR spectra (for U-suc), based on a second order polynomial (Supporting Information, Figure S8). Finally, the recalculated values for ΔE_0 were fixed for the shell fit of each sample. The results of this final fit are shown for the U-ac and the U-suc systems in Figure 7. The

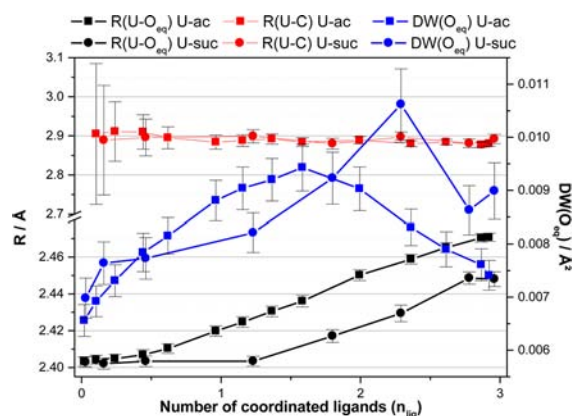


Figure 7. U-O_{eq} distance (black), corresponding DW (blue), and U-C distance (red) as a function of the number of coordinated ligands for the U-ac (filled squares) and U-suc (filled circles) systems.

abscissa is the number of coordinated ligands (n_{lig}) calculated by using eq 1. For the calculation of n_{lig} the relative concentrations of the thermodynamic pH-speciation¹ (Figure 2-C) and the pH-speciation resulting from ITFA on IR spectra (Figure 2-D) were used for the U-ac and the U-suc systems, respectively.

$$n_{\text{lig}} = 1 \cdot [1: 1] + 2 \cdot [1: 2] + 3 \cdot [1: 3] \quad (1)$$

For the following discussions it should be noted that the error of relative changes⁴¹ of bond lengths can be much lower than the absolute error in determination of the bond length ($0.01\text{--}0.02 \text{ \AA}$)⁴² with EXAFS. The relative error depends on the reproducibility of an EXAFS spectrum. To estimate the relative error in determination of relative changes in distances, the 11th sample of the U-ac series was measured four times and the data were fitted separately. The calculated standard deviation of the four fitted distances can serve as a measure of the precision in determination of the relative changes. The

standard deviations are 0.003 Å (O_{eq}), 0.005 Å (C), and 0.012 Å (C_{dis}). Note that the absolute error of the bond length might be validated for the 1:3 U-ac complex by comparison of the structural parameters, given in Table 2, with those from XRD.¹⁸

In the U-ac system, the $U-O_{\text{eq}}$ bond length increases monotonically with the increase of coordinated ligands (Figure 7). The DW increases until an average n_{lig} of 1.6 and then decreases. The lowest values of the DW of O_{eq} are hence observed, when the equatorial shell is fully occupied by waters or by ac ligands, corresponding to uranyl hydrate and the 1:3 U-ac complex, respectively. As uranyl hydrate shows a uniform coordination of water molecules thus having low structural disorder, it is evident that the 1:3 complex shows also a similar uniform coordination of acetate molecules. The highest DW appears at 1.6 coordinated ac ligands which corresponds to pH 2.57 where in average $\sim 2 O_{\text{eq}}$ belong to the coordinated water molecules and $\sim 3 O_{\text{eq}}$ to the carboxylic groups. At this pH, the fractions of the U-ac complexes are distributed nearly equally (33% 1:1 U-ac, 28% 1:2 U-ac, 23% 1:3 U-ac), hence the high DW can be explained by the high structural disorder because of the presence of structurally different complexes as well as by the presence of differently coordinating ligands, like water molecules and acetate ligands, in nearly equal fractions. Unlike the investigations of Jiang et al.,⁵ we found a relatively long $U-O_{\text{eq}}$ distance of ~ 2.47 Å at the highest pH. This is in line with the $U-O_{\text{eq}}$ distance of 2.48 Å for three bidentately coordinated acetate groups in solid $\text{Na}[\text{UO}_2\text{ac}_3]$ measured by EXAFS.¹⁵ This quite simple shell fit approach gives already strong evidence for a bidentate coordination of all acetate groups in the 1:3 U-ac complex. Over the whole pH range and for both systems, the measured U–C distances are in average 2.89 ± 0.01 Å (Figure 7) which is typical for bidentate coordination (EXAFS,^{6,15} XRD¹⁸).

In contrast to the U-ac system, the $U-O_{\text{eq}}$ distance in the U-suc system (Figure 7) remains constant until ~ 1.2 suc ligands are coordinated, and then raises rapidly to a final value of 2.45 Å. The distance is in line with several carboxylic ligands coordinated bidentately. The constant average $U-O_{\text{eq}}$ distance up to one coordinated suc ligand can be explained by a short distance coordination of the carboxyl group in which the suc ligand is coordinated with a $U-O_{\text{eq}}$ distance similar to that observed for uranyl hydrate and/or by water molecules with a shorter $U-O_{\text{eq}}$ distance than in the case of uranyl hydrate. A shortening of the $U-O_{\text{eq}}$ distance of the carboxyl group should cause a shortening of the U–C distances, which, however, is not observed in the present case (Figure 7). Therefore, it is reasonable to assume that a shortening of the $U-O_{\text{eq}}$ distance of coordinated water molecules is responsible for the short average $U-O_{\text{eq}}$ distance up to 1.2 coordinated suc ligands. The DW of O_{eq} rises up to 2.3 coordinated suc ligands and drops down afterward to a final value of $\text{DW} = 0.009 \text{ \AA}^2$ which is higher than that observed for the U-ac system ($\text{DW} = 0.007 \text{ \AA}^2$). Note that the error in determination is high at the DW maximum (Figure 7). Hence, we can not exclude that this point is an outlier. The lower final $U-O_{\text{eq}}$ distance of 2.45 Å and the higher final DW, when compared with the U-ac system, is a first hint that the ligands are not uniformly coordinated in the 1:3 U-suc complex opposite to the uniform coordination in the 1:3 U-ac complex. Several reasons for the reduced $U-O_{\text{eq}}$ distance are possible:

(1) At first, the carboxylic group of succinic acid might connect uranium at a shorter distance in bidentate mode. If one assumes that the bond angles and bond lengths for the carboxyl

group are the same for coordinated ac and suc ligands, then the U–C distance depends only on the $U-O_{\text{eq}}$ distance of the bidentate coordinated carboxyl group. Consequently, the measured U–C distance of 2.89 Å at three coordinated suc ligands will cause a $U-O_{\text{eq}}$ distance slightly longer or equal to the $U-O_{\text{eq}}$ distance measured for U-ac (2.47 Å) where a U–C distance of 2.88 Å was observed in the case of three coordinated ligands. Therefore a short distance bidentate coordination can be ruled out.

(2) Second, one or more suc ligands might be coordinated in “non”-bidentate fashion like monodentate or ring chelate coordination which generally result in shorter $U-O_{\text{eq}}$ distances. Under such circumstances the average $U-O_{\text{eq}}$ distance could be reduced to the measured value of 2.45 Å. However, because of sterical reasons (larger ring chelates show a considerably higher demand for space) it is unlikely that in the case of two bidentately coordinated suc ligands the third suc ligand is coordinated via two carboxylic groups by forming a seven membered ring. Therefore, only a formation of a 1:3 U-suc complex, in which besides of two bidentate coordinated ligands one ligand is coordinated in a monodentate fashion is likely and the average $U-O_{\text{eq}}$ distance would decrease. In addition, if two different binding modes of the carboxylic group are present, the DW would increase because of a higher disorder in the equatorial shell, which would be in line with the observation (Figure 7).

To answer the question about the binding mode in the U-suc system, in the next section ITFA is applied on spectral features such as the $U-C-C_{\text{dis}}-C$ and $U-C-C_{\text{dis}}$ MS paths which are characteristic and an indicator for a bidentate coordination. By using only the average structural parameter for the interpretation of the structures of the complexes (Figure 7), it is difficult to find out how the ligands are coordinated in the 1:1 and 1:2 U-ac and U-suc complexes because they do not occur as major species in solution. ITFA will be applied in the following section on both series of EXAFS spectral mixtures to determine the relative concentrations of the components and to isolate the component spectra from their mixtures.

ITFA of EXAFS Spectra. ITFA was performed with the spectra of the U-ac and the U-suc system (Supporting Information, Figure S9 and Figure S10), while three distinct components were identified in both cases. The ITFA extracted component spectra are shown in Figure 8, and the corresponding pH-speciations are shown together with the VARIMAX factor loadings in Supporting Information, Figure S11. Tables 2 and 3 contain the structural parameters gained by the shell fit for the U-Ac and the U-suc system for each component. For the fit we applied the same fit model explained above with the exception that CN of O_{eq} and C is now freely fitted and that for each system for component 3 the C_{dis} SS path and the corresponding MS paths $U-C-C_{\text{dis}}-C$ and $U-C-C_{\text{dis}}$ were included. The CN of C_{dis} and of the MS path $U-C-C_{\text{dis}}-C$ were set once and the CN of the MS path $U-C-C_{\text{dis}}$ was set twice to the CN of the C atom, respectively. During the fit the effective path lengths of the MS paths were fixed to the value of the freely fitted $U-C_{\text{dis}}$ distance. The DW of C, C_{dis} and of the MS paths was determined by fitting the 1:3 complex of the U-ac system with a constant $\text{CN}_C = 3$, while during the fit for both connected MS paths the DW was set to the value of the freely fitted DW of C_{dis} . The determined DWs for C, C_{dis} and for the $U-C-C_{\text{dis}}-C$ and $U-C-C_{\text{dis}}$ MS paths were then taken as constant values for the final shell fit (Tables

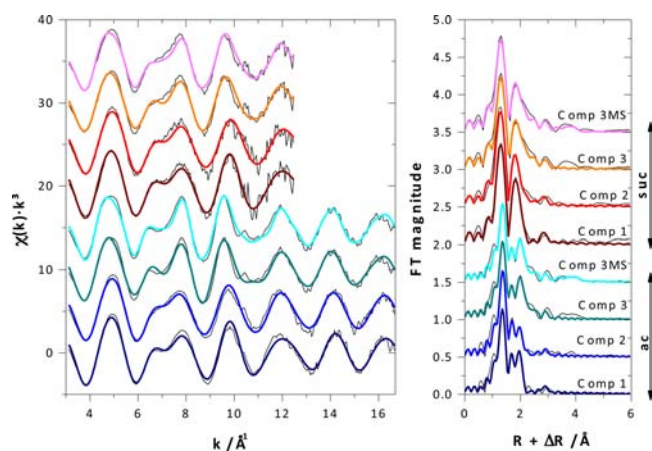


Figure 8. EXAFS spectra and the corresponding Fourier transforms of the extracted components of the U-ac and U-suc systems. The fit of the third component in each system is shown with and without inclusion of the MS paths of the carboxylic group.

Table 3. Shell Fit Parameters for the Extracted Components in the U-suc System

	atom	CN ^a	R[Å] ^b	σ ² [Å ²] ^c	ΔE ₀ [eV] ^d
component 1	O _{ax}	2*	1.764(2)	0.0011(1)	3.3(4)
	O _{eq}	4.9(3)	2.405(4)	0.0064(7)	/3.3
component 2	O _{ax}	2*	1.759(2)	0.0017(2)	3.91*
	O _{eq}	5.7(6)	2.403(5)	0.011(1)	/3.91
	C	1.5(4)	2.90(2)	0.0042*	/3.91
component 3	O _{ax}	2*	1.776(2)	0.0014(1)	4.5(5)
	O _{eq}	5.0(4)	2.449(5)	0.0089(9)	/4.5
	C	2.6(3)	2.888(8)	0.0042*	/4.5
	C _{dis}	/2.6	4.35(1)	0.00645*	/4.5

^aCoordination number. ^bInteratomic distance. ^cDebye–Waller factor. ^dThreshold energy, * fixed parameter, /parameter linked proportional to the parameter in the row above. CN ± ~20%, R ± ~0.02 Å. The standard deviations of the variable parameters as estimated by EXAFSPAK are given in parentheses. MS O_{ax} and both MS paths of C_{dis} were linked to the structural parameters of O_{ax} and SS C_{dis} accordingly.

2 and 3). For both systems the C_{dis} and the connected MS paths were only fitted for component 3.

For both systems component 1 (Table 2 and Table 3) shows nearly the same structural parameters. The U–O_{eq} distance of 2.40 Å is typical for water coordination, and the low DW of ~0.006–0.007 Å² points out that the O_{eq} shell shows uniform coordination. Therefore, component 1 can be assigned to uranyl hydrate in accordance with the IR and UV–vis results. Component 2 shows for both systems only slightly different U–O_{eq} distances compared to uranyl hydrate. In contrast, the DW of O_{eq} is raised to 0.011 Å² in both systems pointing out that at least two different types of O_{eq} atoms are present. Component 3 shows an elongated U–O_{eq} distance for both systems. Moreover, the U–O_{eq} distances and the corresponding DWs are comparable to those that were already visible in Figure 7 at *n*_{lig} ~ 3. Hence, this component can be mainly assigned to the 1:3 complexes in each system.

An assignment of the components can be also done by comparing the ITT determined pH-speciations based on the EXAFS spectra (Supporting Information, Figure S11–C (U-ac) and Supporting Information, Figure S11–D (U-suc)) with the pH-speciations determined by using IR (Figure 2–C (U-ac) and

Figure 2–D (U-suc)) and UV–vis spectroscopy (Supporting Information, Figure S7–C (U-ac) and Supporting Information, Figure S7–D (U-suc)). For both systems the best match is observed between component 1 and uranyl hydrate, component 2 and the 1:1 complex and between component 3 and the 1:3 complex.

Figure 9 shows the speciation distribution of the extracted components of the U-ac system compared with the speciation

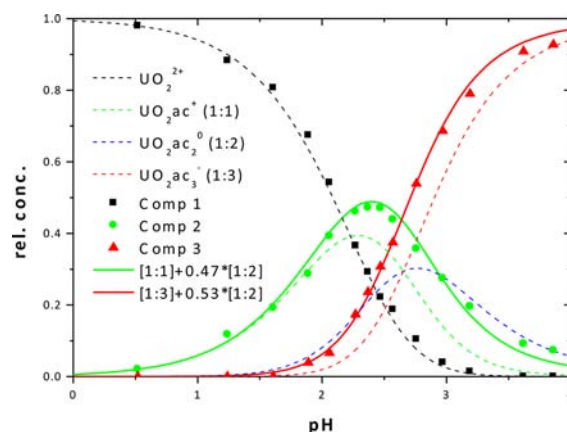


Figure 9. pH dependence of U(VI) speciation under 50 mM U(VI) and 1 M acetic acid. Relative fractions of the complexes according to thermodynamic speciation calculation¹ (dotted lines), ITT derived relative concentrations of the components (points), and relative concentrations of the components calculated by using the thermodynamical speciation calculation¹ after distributing the 1:2 complex over the 1:1 and 1:3 complexes (solid lines).

calculated using the complex stability constants reported by Ahrlund.¹ The question arises why only three components were identified in the case of EXAFS whereas the ITFA applied on UV–vis and IR yielded four components. An intrinsic property of factor analysis is that only the components which are linear independent to each other are detectable. In other words, if a spectrum of a certain complex can be reproduced by a linear combination of the spectra of two (or more) other complexes present in the spectral mixtures, then this complex is not detectable as a component. Hence the number of estimated components becomes less than the number of the acting complexes. If one complex is missing, then its fraction adds to the fractions of the other complexes whose spectra can reproduce the spectrum of this complex by their linear combination. Because of this behavior the relative concentrations of the complexes, which enable the reproduction of the spectrum of the missing complex, are enhanced and are shifted toward the position of the missing complex. To figure out which complex is invisible by factor analysis, a comparison of the IR- and UV–vis-supported thermodynamic pH-speciation¹ with the pH-speciation of the three components is instructive (Figure 9). The speciation of uranyl hydrate (component 1) is not affected, while the 1:1 U-ac (component 2) and the 1:3 U-ac complexes (component 3) are shifted toward the 1:2 complex. Therefore, we can assume that the 1:2 complex is the missing complex. By using this hypothesis and the assumption that the spectrum of the 1:2 complex (*sp*_{1:2}) can be reproduced with the spectra of the 1:1 (*sp*_{1:1}) and the 1:3 complex (*sp*_{1:3}) with eq 2:

$$sp_{1:2} = a \cdot sp_{1:1} + (1 - a) \cdot sp_{1:3} \quad (2)$$

the relative concentrations of the components 2 and 3 can be calculated solely on the basis of the thermodynamically calculated relative concentrations of the 1:1, 1:2, and 1:3 complexes¹ by eq 3:

$$\begin{aligned} [\text{component2}] &= [1: 1] + a \cdot [1: 2] \\ [\text{component3}] &= [1: 3] + (1 - a) \cdot [1: 2] \end{aligned} \quad (3)$$

Figure 9 shows a comparison of the thermodynamically derived speciation with that from ITT. The value of the factor, a , was found to be $a = 0.47$ by minimizing the RMS error between relative concentrations of the thermodynamically derived and the ITFA derived components. The good match in the relative concentrations of the complexes calculated using two different methods is a proof of the validity of our hypothesis and assumptions (Figure 9). Accordingly, the ITFA isolated spectra of component 2 and component 3 are confirmed to be those of the 1:1 and 1:3 complexes, respectively.

The obtained value of factor a is nearly one-half. This points out that the missing complex should be composed to one-half of the 1:1 complex and to one-half of the 1:3 complex. Consequently, the missing complex should be the 1:2 complex. In addition, this indirect proof of the complex stoichiometry shows that the results gained by all used spectroscopies are consistent. These results show that the 1:2 complex must consist of the same structural entities as present in the 1:1 (component 2) and 1:3 (component 3) complexes, that is, O_{ax} coordinated water molecules, and bidentately coordinated ac ligands. Moreover, the EXAFS signals stemming from the coordinated atoms and ligands must be similar within the 1:1, 1:2, and 1:3 complexes; hence, the radial distances and DWs of these spectral contributions are similar among these complexes. If for instance the water molecules and/or the carboxylic group would be coordinated in a different radial distance for one of these complexes then it would be impossible to calculate the spectrum of the 1:2 complex by the linear combination of the spectra of the 1:1 and 1:3 complexes.

In contrast to the other components, the ITT derived relative concentrations of component 1 (uranyl hydrate) match the relative concentrations determined by thermodynamical calculations (Figure 9) closely; hence, the spectral contributions of O_{ax} and/or coordinated water molecules and therefore the structural parameters of these contributions do not match those present in the U-ac complexes. The variation of the spectral contribution of O_{ax} within the pH series is of minor importance when compared with the spectral variations caused by structural changes in the equatorial plane of U(VI) (Supporting Information, Figure S9). This suggests that mainly the spectral contribution of the uranyl hydrate water molecules does not fit the spectral contributions of the coordinated water molecules in the 1:1 and 1:2 complexes. In other words the spectral contribution of coordinated water molecules and therefore the radial $U-O_{\text{eq}}$ distance, as the most sensitive structural parameter, are different between the uranyl hydrate and the 1:1 and 1:2 complexes. This assumption can be verified by calculating the $U-O_{\text{eq}}$ distances in the 1:1 complex in the following way. The measured $U-O_{\text{eq}}$ distance for the coordinated water molecule is $R(U-O_{\text{eq}}) = 2.40 \text{ \AA}$ in uranyl hydrate (component 1, Table 2), and the $U-O_{\text{eq}}$ distance for the carboxylic group is $R(U-O_{\text{eq}}) = 2.47 \text{ \AA}$ in the 1:3 complex (component 3, Table 2). Assuming that the $R(U-O_{\text{eq}}) = 2.40 \text{ \AA}$ for water oxygen and $R(U-O_{\text{eq}}) = 2.47 \text{ \AA}$ for carboxyl

oxygen retain also in the 1:1 complex, the expected average $U-O_{\text{eq}}$ distance for the 1:1 complex (CN = 5, bidentate) is 2.43 \AA , while we obtained a relative shorter distance of 2.41 \AA (component 2, Table 2). This is a first indication that for the ac complexes the $U-O_{\text{eq}}$ distance of coordinated water molecules might be shorter than that observed for uranyl hydrate. The $U-O_{\text{eq}}$ distance of the water molecules coordinated at shorter distance can be calculated by taking the measured average $U-O_{\text{eq}}$ distance of 2.41 \AA for the 1:1 complex (component 2, Table 2) and that of 2.47 \AA for the 1:3 complex (component 3, Table 2) to $R(U-O_{\text{eq}}) = (5 \cdot 2.41 \text{ \AA} - 2 \cdot 2.47 \text{ \AA})/3 = 2.37 \text{ \AA}$. This uranium-to-water distance is 0.03 \AA shorter than that in uranyl hydrate.

As the next step of analysis, we developed a method to calculate the $U-O_{\text{water}}$ and $U-O_{\text{carboxylate}}$ distances for the 1:1 and 1:2 complexes, separately. This method is described in detail in the Supporting Information. The determined optimum distances for the 1:1 and the 1:2 complexes are $R(U-O_{\text{water}}) = 2.350 \text{ \AA}$ and $R(U-O_{\text{carboxylate}}) = 2.465 \text{ \AA}$. In line with the DFT calculations and especially in the case of the 1:1 complex, the goodness-of-fit value is lower for a 5-fold than for a 6-fold coordination. The shorter $U-O_{\text{water}}$ distance, observed for the 1:1 and 1:2 complexes, is supported by the crystal structure of $UO_2ac_2 \cdot 2H_2O$ showing $R(U-O_{\text{water}}) = 2.34 \text{ \AA}$.⁴³

Also in the U-suc system, a simple theoretical calculation of the average $U-O_{\text{water}}$ distance of the 1:1 complex can be done using the assumption that the measured O_{eq} distance of the 1:1 complex (component 2) is the weighted average of $U-O_{\text{water}}$ and $U-O_{\text{carboxylate}}$. The $U-O_{\text{carboxylate}}$ distance can be set to the value obtained for the single component of the U-ac 1:3 complex (component 3, Table 2), and the average distance of the 1:1 U-suc complex is taken from component 2 in Table 3. In the case of 5-fold coordination $R(U-O_{\text{water}}) = (5 \cdot 2.40 \text{ \AA} - 2 \cdot 2.47 \text{ \AA})/3 = 2.35 \text{ \AA}$. The average $U-O_{\text{water}}$ distance is again much smaller than that of uranyl hydrate and would be again comparable to $R(U-O_{\text{water}})$ in $UO_2ac_2 \cdot 2H_2O$.⁴³

A similar calculation using theoretical spectra as in the case of the U-ac system was used to find the optimum distances. For the 1:1 complex and in the case of CN = 5 the resulting distances are $R(U-O_{\text{water}}) = 2.355 \text{ \AA}$ and $R(U-O_{\text{carboxylate}}) = 2.455 \text{ \AA}$.

The $U-O_{\text{eq}}$ distance of the 1:3 U-suc complex (Table 3) is by 0.02 \AA shorter than the $U-O_{\text{carboxyl}}$ distance of 2.47 \AA measured in the case of the 1:3 U-ac complex (Table 2). With the assumption that the structure of the carboxylic group is the same for suc and ac then in the case of the 1:3 U-suc complex the carboxylic groups should coordinate in a $U-O_{\text{carboxyl}}$ distance similar to that of the 1:3 U-ac complex because the measured $U-C$ distance is similar to that of the 1:3 U-ac complex (compare component 3 in Table 2 and Table 3). One simple explanation for the smaller $U-O_{\text{eq}}$ distance in the case of the 1:3 suc complex would be that one suc ligand is coordinated in a monodentate fashion with a distance of $R(U-O_{\text{monodentate}}) < R(U-O_{\text{bidentate}})$. In such situation the average $U-O_{\text{eq}}$ distance would decrease relative to the $U-O_{\text{bidentate}}$ distance which would be in line with the observation.

Furthermore, the CN of the $U-C-C_{\text{dis}}-C$ and $U-C-C_{\text{dis}}$ MS paths can be taken as a measure of the number of bidentately coordinated carboxyl groups (CN(bidentate)). The CN of monodentately coordinated ligands is the difference between the known CN of the coordinated ligands and CN(bidentate). The CN of these MS paths could be determined by a shell fit. Unfortunately, the DWs of the MS

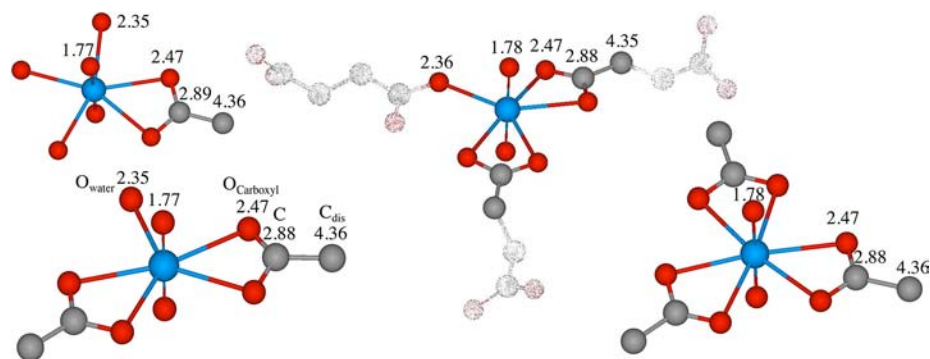


Figure 10. Proposed structures of the 1:1, 1:2, and 1:3 complexes in the U-ac system and the 1:3 U-suc complex. Radial distances are given in angstrom (Å). (Blue, uranium; red, oxygen; gray, carbon; hydrogen atoms are omitted for clarity. Gray shaded atoms are not visible using EXAFS spectroscopy.

paths are not known a priori and also correlate with the CNs so that both parameters, the CN and the DW, must be fitted at the same time which can cause uncertainties in determination. Another way is the use of ITFA which solely with the experimental data enables a direct quantification of the U–C–C_{dis} MS paths without fitting. This was done by analyzing the Fourier-backtransform of the EXAFS signal of the U–C–C_{dis}–C and U–C–C_{dis} MS paths with ITFA (see Supporting Information). For the 1:3 U-suc complex the resulting number of bidentate coordinated carboxylic groups is CN(bidentate) = 2.04 (Supporting Information, Figure S17); this is a value which enables the conclusion that in the 1:3 U-suc complex one of the three suc ligands is coordinated in monodentate fashion which is in line with the explanation of the shorter U–O_{eq} distance and the higher DW of O_{eq} when compared with a uniform bidentate coordination in the 1:3 U-ac complex.

To get information about the coordination of the other complexes in the U-suc system, a theoretical CN(bidentate) was calculated by multiplying the ITT determined relative concentrations of the components (Supporting Information, Figure S11-D) with the number of assumed CN(bidentate). Two models were compared with each other, while for both models for component 3 (1:3 complex) the CN(bidentate) = 2. In the case of model 1 one bidentate (CN(bidentate) = 1) and for model 2 one monodentate (CN(bidentate) = 0) coordinated suc ligand was assumed for the component 2 (1:1 complex). For model 1 the lowest standard deviation (SD) between the theoretical and the ITT calculated CN(bidentate) is observed (Supporting Information, Figure S17). This would be in line with the IR results which suggest mainly bidentate coordination up to pH 3, hence for the 1:1 and 1:2 U-suc complexes (Figure 2-D).

Finally the question can be answered why also in the case of the U-Suc system the 1:2 complex is not detectable with ITFA. In principle, three cases for the coordination in the 1:2 complex are possible: (a) two bidentate, (b) one bidentate and one monodentate, and (c) two monodentate coordinated suc ligands. The case (c) can be discarded because the spectrum of such a complex would not be a linear combination of the 1:1 and 1:3 complexes which contain at least one or two bidentate coordinated suc ligands, respectively. The spectral contribution of the monodentately coordinated carboxylic group ($R(\text{U}-\text{O}_{\text{eq}}) = 2.35 \text{ \AA}^5$) in the 1:3 complex is expected to be similar to the spectral contribution of coordinated water molecule/s in the 1:1 or the 1:2 complexes ($R(\text{U}-\text{O}_{\text{eq}}) \sim 2.36 \text{ \AA}$). Concerning this spectral similarity for case (a) the spectrum

of the 1:2 complex would be similar to the spectrum of the 1:3 complex, while for case (b) the spectrum of the 1:2 complex would be similar to the spectrum of the 1:1 complex. Moreover, the spectrum of the 1:2 complex must agree within the experimental error with the spectrum of the 1:3 complex or the 1:1 complex, because only three components were detected by ITFA. According to the results gained from the IR, case (a) might be the preferred solution for the 1:2 complex, hence a bidentate coordination of the two suc ligands, but at the current stage of the investigations it cannot be ruled out that one bidentate and one monodentate coordinated suc ligand is present in the 1:2 complex.

SUMMARY

In the case of the U-ac system the thermodynamic model of Ahrlund¹ was validated by the application of ITFA on IR and UV–vis spectra. With increasing pH, complexes of the following stoichiometry occur: 1:0, 1:1, 1:2, and 1:3. The U-ac complexes show exclusively bidentate coordination as evidenced by (1) monotonically increasing U–O_{eq} bond length (from 2.40 Å for uranyl hydrate to $\sim 2.47 \text{ \AA}$ for the 1:3 complex) and increasing number of coordinated ligands with increasing pH, (2) a decrease of the spectral splitting ($\Delta\nu$) of the $\nu_{3,s}(\text{COO})$ and the $\nu_{3,as}(\text{COO})$ mode from 136 (acetate ion) to 70 cm^{-1} (U-ac complex), and (3) the absence of any feature in the region around 1580 cm^{-1} that might be assigned to the $\nu_{3,as}(\text{COO})$ mode of monodentate coordination. The shift of the $\nu_3(\text{UO}_2)$ mode follows the stepwise coordination of acetate ligands: 961 cm^{-1} → uranyl hydrate, 949 cm^{-1} → 1:1 complex, 939 cm^{-1} → 1:2 complex, and 924 cm^{-1} → 1:3 complex. These experimental vibrational frequencies are in line with the DFT-calculated values. According to the DFT calculations only the 1:3 complex is 6-fold coordinated, while the remaining complexes are 5-fold coordinated. In contrast to IR and UV–vis spectroscopy, factor analysis of the EXAFS data resulted in only 3 different components. The extracted components were uranyl hydrate, the 1:1 complex, and the 1:3 complex while the spectrum of 1:2 complex is reproducible by a linear combination of the spectra of the 1:1 and 1:3 complexes. In line with the solid complex of $\text{Na}[\text{UO}_2\text{ac}_3]$ ¹⁵ the 1:3 complex showed U–O_{eq}, U–C, and U–C_{dis} distances of 2.47, 2.88, and 4.36 Å, respectively. A combination of ITFA with theoretical spectra indicated for the 1:1 and the 1:2 complexes that the coordinated water molecules are closer to the uranyl ion (2.35 Å) than in the case of the uranyl hydrate (2.40 Å).

In the U-suc system, four components were found by applying ITFA on the IR and UV-vis data. However, the calculated speciation pattern was not in line with previously published thermodynamic data. Moreover, DFT calculation showed that the observed stepwise shift of the $\nu_3(\text{UO}_2)$ mode can only be interpreted with the existence of the 1:3 complex that was previously unreported. In analogy to the U-ac system, a decrease of $\Delta\nu$ from 152 (succinate ion) to 72 cm^{-1} (U-suc complex) was found to indicate the dominance of bidentate coordination. A broad water band disturbed the spectra in the region around 1580 cm^{-1} where contributions from the $\nu_{3,\text{as}}(\text{COO})$ mode of monodentately coordinated ligand molecules might be present. ITFA applied on the EXAFS spectral series showed only three components: Uranyl hydrate, 1:1 complex, and an 1:3 complex. The spectrum of the 1:2 complex can be formed by a linear combination of the spectra of the other complexes and is therefore not detectable by ITFA. The 1:3 U-suc complex has an average U-O_{eq} distance of 2.45 Å which is clearly shorter than that in the 1:3 U-ac complex pointing out that at least one carboxylic group did not show bidentate coordination. The inspection of the MS paths along the U-C-C_{dis} chain pointed out that in the case of the 1:1 complex one carboxylic group is coordinated in a bidentate mode, while in the 1:3 complex two carboxylic groups coordinate bidentately and one monodentately.

Figure 10 shows the discussed structure of the 1:3 U-suc complex and all the structures of the U-ac complexes.

■ ASSOCIATED CONTENT

● Supporting Information

Speciation calculation, sample composition, information about the application of FA, DFT calculated band positions of the U-suc system, UV-vis spectra for both series including VARIMAX and ITT results, recalculation of the threshold energy, EXAFS spectra for all samples including VARIMAX and ITT results, picture of the FEFF model, method of calculation of $R(\text{U}-\text{O}_{\text{water}})$ and $R(\text{U}-\text{O}_{\text{carboxyl}})$ with surface plots of the resulting local minima, and Fourier filtered EXAFS spectra of the U-C_{dis} path and the U-C-C_{dis} MS paths in the U-suc system. This material is available free of charge via the Internet at <http://pubs.acs.org>.

■ AUTHOR INFORMATION

Corresponding Author

*E-mail: c.lucks@hzdr.de (C.L.), rossberg@esrf.fr (A.R.).

Notes

The authors declare no competing financial interest.

■ ACKNOWLEDGMENTS

This study was supported by the Deutsche Forschungsgemeinschaft (DFG) under contract number RO 2254/3-1. The authors acknowledge generous allocation of CPU time on the supercomputer at the Zentrum für Informationsdienste und Hochleistungsrechnen (ZIH), Technische Universität Dresden, Germany. The authors gratefully acknowledge the help of K. Heim for the acquisition of IR data and the help of A. Ikeda-Ohno for preparation of the U-ac EXAFS samples.

■ REFERENCES

- (1) Ahrland, S. *Acta Chem. Scand.* **1951**, *5* (2), 199–219.
- (2) Stary, J. *Collect. Czech. Chem. Commun.* **1960**, *25* (10), 2630–2641.
- (3) Miyake, C.; Nurnberg, H. W. *J. Inorg. Nucl. Chem.* **1967**, *29* (9), 2411–2429.
- (4) Portanova, R.; Di Bernardo, P.; Cassol, A.; Tondello, E.; Magon, L. *Inorg. Chim. Acta* **1974**, *8* (2), 233–240.
- (5) Jiang, J.; Rao, L. F.; Di Bernardo, P.; Zanonato, P.; Bismondo, A. *J. Chem. Soc., Dalton Trans.* **2002**, *8*, 1832–1838.
- (6) Bailey, E. H.; Mosselmans, J. F. W.; Schofield, P. F. *Geochim. Cosmochim. Acta* **2004**, *68* (8), 1711–1722.
- (7) Kakihana, M.; Nagumo, T.; Okamoto, M.; Kakihana, H. *J. Phys. Chem.* **1987**, *91* (24), 6128–6136.
- (8) Quiles, F.; Burneau, A. *Vib. Spectrosc.* **1998**, *18* (1), 61–75.
- (9) Gal, M.; Goggin, P. L.; Mink, J. *Spectrochim. Acta, Part A* **1992**, *48* (1), 121–132.
- (10) Nguyen-Trung, C.; Begun, G. M.; Palmer, D. A. *Inorg. Chem.* **1992**, *31* (25), 5280–5287.
- (11) Malinowski, E. R. *Factor Analysis in Chemistry*, 2nd ed.; John Wiley & Sons: New York, 1991.
- (12) Rossberg, A.; Reich, T.; Bernhard, G. *Anal. Bioanal. Chem.* **2003**, *376* (5), 631–638.
- (13) Kaiser, H. F. *Psychometrika* **1958**, *23* (3), 187–200.
- (14) Brayden, T. H.; Poropatic, P. A.; Watanabe, J. L. *Anal. Chem.* **1988**, *60* (11), 1154–1158.
- (15) Denecke, M. A.; Reich, T.; Bubner, M.; Pompe, S.; Heise, K. H.; Nitsche, H.; Allen, P. G.; Bucher, J. J.; Edelstein, N. M.; Shuh, D. K. *J. Alloys Compd.* **1998**, *271*, 123–127.
- (16) Allen, P. G.; Bucher, J. J.; Shuh, D. K.; Edelstein, N. M.; Reich, T. *Inorg. Chem.* **1997**, *36* (21), 4676–4683.
- (17) Hennig, C.; Tutschku, J.; Rossberg, A.; Bernhard, G.; Scheinost, A. C. *Inorg. Chem.* **2005**, *44* (19), 6655–6661.
- (18) Templeton, D. H.; Zalkin, A.; Ruben, H.; Templeton, L. K. *Acta Crystallogr., Sect. C: Cryst. Struct. Commun.* **1985**, *41* (OCT), 1439–1441.
- (19) Vallet, V.; Moll, H.; Wahlgren, U.; Szabo, Z.; Grenthe, I. *Inorg. Chem.* **2003**, *42* (6), 1982–1993.
- (20) Rao, L. F.; Jiang, J.; Zanonato, P. L.; Di Bernardo, P.; Bismondo, A.; Garnov, A. Y. *Radiochim. Acta* **2002**, *90* (9–11), 581–588.
- (21) Burns, P. C.; Ewing, R. C.; Hawthorne, F. C. *Can. Mineral.* **1997**, *35*, 1551–1570.
- (22) Deacon, G. B.; Phillips, R. J. *Coord. Chem. Rev.* **1980**, *33* (3), 227–250.
- (23) Groenewold, G. S.; de Jong, W. A.; Oomens, J.; Van Stipdonk, M. J. *J. Am. Soc. Mass Spectrom.* **2010**, *21* (5), 719–727.
- (24) Bismondo, A.; Cassol, A.; Di Bernardo, P.; Magon, L.; Tomat, G. *Inorg. Nucl. Chem. Lett.* **1981**, *17* (3–4), 79–81.
- (25) Rawat, N.; Tomar, B. S.; Manchanda, V. K. *J. Chem. Thermodyn.* **2011**, *43* (7), 1023–1027.
- (26) Matz, W.; Schell, N.; Bernhard, G.; Prokert, F.; Reich, T.; Claussner, J.; Oehme, W.; Schlenk, R.; Diemel, S.; Funke, H.; Eichhorn, F.; Betzl, M.; Prohl, D.; Strauch, U.; Huttig, G.; Krug, H.; Neumann, W.; Brendler, V.; Reichel, P.; Denecke, M. A.; Nitsche, H. *J. Synchrotron Radiat.* **1999**, *6*, 1076–1085.
- (27) George, G. N.; Pickering, I. J. *EXAFSPAK: A Suite of Computer Programs for Analysis of X-ray Absorption Spectra*; Stanford Synchrotron Radiation Laboratory: Stanford, CA, 1995.
- (28) Ankudinov, A. L.; Ravel, B.; Rehr, J. J.; Conradson, S. D. *Phys. Rev. B.* **1998**, *58* (12), 7565–7576.
- (29) Frisch, M. J.; Trucks, G. W.; Schlegel, H. B.; Scuseria, G. E.; Robb, M. A.; Cheeseman, J. R.; Montgomery, J. J. A.; Vreven, T.; Kudin, K. N.; Burant, J. C.; Millam, J. M.; Iyengar, S. S.; Tomasi, J.; Barone, V.; Mennucci, B.; Cossi, M.; Scalmani, G.; Rega, N.; Petersson, G. A.; Nakatsuji, H.; Hada, M.; Ehara, M.; Toyota, K.; Fukuda, R.; Hasegawa, J.; Ishida, M.; Nakajima, T.; Honda, Y.; Kitao, O.; Nakai, H.; Klene, M.; Li, X.; Knox, J. E.; Hratchian, H. P.; Cross, J. B.; Bakken, V.; Adamo, C.; Jaramillo, J.; Gomperts, R.; Stratmann, R. E.; Yazyev, O.; Austin, A. J.; Cammi, R.; Pomelli, C.; Ochterski, J. W.; Ayala, P. Y.; Morokuma, K.; Voth, G. A.; Salvador, P.; Dannenberg, J. J.; Zakrzewski, V. G.; Dapprich, S.; Daniels, A. D.; Strain, M. C.; Farkas, O.; Malick, D. K.; Rabuck, A. D.; Raghavachari, K.; Foresman, J. B.; Ortiz, J. V.; Cui, Q.; Baboul, A. G.; Clifford, S.; Cioslowski, J.

Stefanov, B. B.; Liu, G.; Liashenko, A.; Piskorz, P.; Komaromi, I.; Martin, R. L.; Fox, D. J.; Keith, T.; Al-Laham, M. A.; Peng, C. Y.; Nanayakkara, A.; Challacombe, M.; Gill, P. M. W.; Johnson, B.; Chen, W.; Wong, M. W.; Gonzalez, C.; Pople, J. A. *Gaussian 03*, Revision E.01; Gaussian, Inc.: Wallingford, CT, 2004.

(30) Barone, V.; Cossi, M. *J. Phys. Chem. A* **1998**, *102* (11), 1995–2001.

(31) Bondi, A. *J. Phys. Chem.* **1964**, *68* (3), 441–451.

(32) Küchle, W.; Dolg, M.; Stoll, H.; Preuss, H. *J. Chem. Phys.* **1994**, *100* (10), 7535–7542.

(33) Bergner, A. *Mol. Phys.* **1993**, *80* (6), 1431–1441.

(34) Macak, P.; Tsushima, S.; Wahlgren, U.; Grenthe, I. *Dalton Trans.* **2006**, *30*, 3638–3646.

(35) Krishnan, R.; Binkley, J. S.; Seeger, R.; Pople, J. A. *J. Chem. Phys.* **1980**, *72* (1), 650–654.

(36) Müller, K.; Brendler, V.; Foerstendorf, H. *Inorg. Chem.* **2008**, *47* (21), 10127–10134.

(37) Suzuki, M.; Shimanouchi, T. *J. Mol. Spectrosc.* **1968**, *28*, 394–410.

(38) Tsushima, S. *Dalton Trans.* **2011**, *40* (25), 6732–6737.

(39) Meinrath, G. *J. Radioanal. Nucl. Chem.* **1996**, *211* (2), 349–362.

(40) Roscoe, B. A.; Hopke, P. K. *Anal. Chim. Acta* **1981**, *132* (DEC), 89–97.

(41) Purans, J.; Timoshenko, J.; Kuzmin, A.; Dalba, G.; Fornasini, P.; Grisenti, R.; Affy, N. D.; Rocca, F.; De Panfilis, S.; Ozhogin, I.; Tiutiunnikov, S. I. Femtometer accuracy EXAFS measurements: isotopic effect in the first, second and third coordination shells of germanium. In *Proceedings of the 14th International Conference on X-Ray Absorption Fine Structure*, Camerino, Italy, July 26–31, 2009; IOP Publishing Ltd.: Bristol, U.K., **2009**; Vol. 190.

(42) Li, G. G.; Bridges, F.; Booth, C. H. *Phys. Rev. B* **1995**, *52* (9), 6332–6348.

(43) Howatson, J.; Grev, D. M.; Morosin, B. *J. Inorg. Nucl. Chem.* **1975**, *37*, 1933–1935.